

Multiband Sensing for Area Recovery

Shridhar Mubaraq Mishra
Department of Electrical Engineering
and Computer Science
University of California
Berkeley, California 94704
Email: smm@eecs.berkeley.edu

Anant Sahai
Department of Electrical Engineering
and Computer Science
University of California
Berkeley, California 94704
Email: sahai@eecs.berkeley.edu

Abstract—Cognitive radios are being proposed for recovering unused spectrum holes in time and space. Unfortunately the metric of detection-sensitivity while being useful for algorithm designers is not indicative of a system’s ability to recover spectrum holes (especially spectrum holes in space). In this paper we extend the safety and performance metrics of Fear of Harmful Interference (F_{HI}) and Probability of Finding a Hole (P_{FH}) from single primary on a single tower to multiple primaries on multiple towers. We show how a simple multiband algorithm which dynamically computes the detection threshold based on sensed power in multiple bands can recover significantly more area than a singleband detector which makes decisions based on in-band information. Effectively Multiband detection acts as a proxy for increasing the number of users.

I. INTRODUCTION

Measurements indicating low spectrum utilization bring to the forefront the inefficiency of the current regulatory regime [1]–[3]. Current regulation specifies spectrum usage on the spatial scale of countries and continents and on temporal scales of years to decades. This leads to poor utilization of spectrum, since the large allocation scale is too conservative and does not coincide well with realities on the ground – wireless systems can operate on much smaller spatial and temporal scales than regulation can efficiently specify. Hence cognitive radios have been proposed to reuse unutilized spectrum in an opportunistic manner by sensing the primary user and using the spectrum only if the frequency band is deemed empty [1].

To realize the vision of cognitive radios, research has been focussed on two fronts. Research on the physical layer has been on new and robust techniques in spectrum sensing to improve the detection sensitivity [4], [5]¹. Research in the MAC/Network layer on the other hand, has been focussed on providing guaranteed service across a given geographic region [6]. For example, the Wireless Rural Area Network (WRAN) system envisioned by the IEEE 802.22 Working Group aims to provide wireless connectivity to users in the TV bands using base stations with cell radius of 30-40km [7]. This service must be provided while ensuring that passive TV receivers at the edge of the coverage area are not interfered

with. Hence the objective of the MAC/Network layer is in maintaining a set of free channels at every location that can be used to provide service guarantees. It is important to understand that the MAC/Network layer’s Quality Of Service (QoS) metrics may not be expressible as a single detection sensitivity metric. In fact, very sensitive detectors may be detrimental to achieving the target QoS.

For example, a very sensitive cognitive radio in Berkeley, California may be able to detect TV transmissions from Sutro tower in San Francisco, from the TV transmitter at Mount San Bruno and from the Fremont tower [8]. So does that mean that this radio is necessarily excluded from using all these channels? For some channels (the channels from Sutro tower are an example of this), the radio can obviously cause interference to potential TV receivers but for other channels the radio can transmit without causing interference. The detection-sensitivity approach is not synergistic to the overall problem of recovering spectrum real estate.

The above discussion necessitates two questions: what are the appropriate metrics to measure the performance of a detector and what detection techniques enable us to perform well under these metrics?. These questions form the core of this paper. In terms of new detection techniques we are interested in assisted/calibrated detection. Currently, detection sensitivity is usually specified assuming worst case channel models. In better-than-worse-case situations these specifications are too conservative leading to the loss of precious spectrum real estate [9]. In assisted/calibrated detection we wish to overcome these losses by using information about our environment. One form of calibration is to use other TV signals to get an estimate of a radio’s shadowing environment. We shall call this detection technique as *multiband sensing*.

Multiband sensing is particularly useful in the case of TV signals where a single tower can house a number of channels. Sutro tower in San Francisco has antennas for 9 Analog TV transmissions, 5 FM transmissions and 10 Digital TV transmissions [8]. After compensating for differences in transmit power, the energy sensed from these channels can be expected to be heavily correlated. Furthermore, proximity

¹We define detection sensitivity as the minimum SNR at which a signal can be reliably detected at a given Probability of Detection (P_D) and Probability of False Alarm (P_{FA}) in a given sensing time

to one tower can be used to infer distance from other towers.

In [10] we showed the gains from multiband sensing using a very simple model of a primary co-located with an anchor transmitter (the anchor transmitter was always 'on'). Gains could be had when the primary was 'off' since we could adjust the detection threshold for the primary based on the received power from the anchor. However, in [10] we did not have appropriate metrics to quantify the real gains from multiband sensing. Furthermore, the paper was focussed on gains at the no-talk radius of a single tower. In this paper we will address the issues of detecting multiple primaries on multiple towers.

The main contributions of this paper are as follows:

- We extend the metrics of Fear of Harmful Interference (F_{HI}) and Probability of Finding a Hole (P_{FH}) to the multi tower multi channel case. These metrics were originally proposed in [9] for a single tower single channel case. These metrics enable us to evaluate cooperation and multiband detection. These techniques are aimed at **reducing target detection sensitivity** and hence cannot be evaluated using the detection sensitivity metric.
- We propose a shadowing model that is a reflection of reality. We break up shadowing into two components: Global shadowing and Local shadowing. Primaries on the same tower suffer similar global shadowing. Multipath for co-located primaries is independent and local shadowing is essentially direction agnostic.
- We propose a simple multiband algorithm for a two tower scenario that dynamically adjusts its detection threshold based on measured signal strengths from multiple primaries housed on multiple towers. Such an algorithm enables us to reclaim spectrum holes in the vicinity of one tower (called tower A) as shown in Figure 1.

The rest of the paper is organized as follows: In Section II we present the multiband problem. We also we introduce a new model for shadowing and multipath that takes into account relevant environmental effects. Next in Section III we introduce Fear of Harmful Interference (F_{HI}) and Probability of Finding a Hole (P_{FH}) for evaluating the performance of various multi-primary multi-tower detection algorithms. In Section IV we shall present a simple multi-band detection algorithm. Finally in Section V we look at the performance of the multiband algorithm as compared it to the performance of the singleband algorithm.

II. PROBLEM SETUP

In this section we setup the multiband problem. For simplicity we will focus on a two tower scenario to illustrate the gains. This setup is explained in Section II-A. The proposed model for shadowing is introduced in Section II-B. We shall

also introduce all the notation to be used in the rest of the paper.

A. Two Tower Setup

For simplicity we shall use the following two tower model as shown in Figure 2 to examine the gains from multiband sensing.

- The tower A is tower at location $(0,0)$. This tower houses C_A primaries/channels. All channels on this tower have the same transmit power P . We also assume symmetric fading distributions for all channels which means that all channels have the same no-talk radius².
- We introduce one additional tower, tower B which houses C_B primaries. Such a model is generally representative of reality; for most towers there is almost one tower that is close enough to impact the detection process.
- Tower B is at a distance $2r_n + D$ from tower A where $D \sim Exp(\eta)$. The angular location of tower B is Uniform $[0, 2\pi)$. Notice that we make the simplifying assumption that the no-talk radius of the two towers do not intersect.
- A cluster of N users is located at a distance of r_A from tower A at coordinates $(r_A, 0)$. The distance of this cluster is r_B from tower B .
- We assume that all the channels are 'on'.

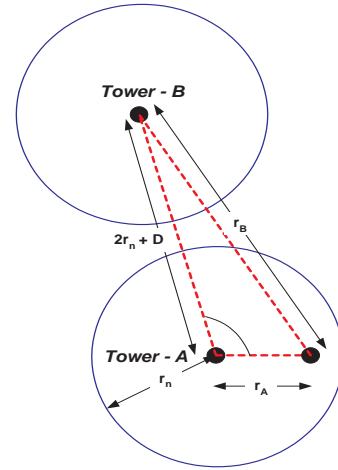


Fig. 2. Model for the placement of towers. Tower A is centered at the origin. A cluster of N users are located at a distance r_A from this tower. This cluster is at a distance of r_B from tower B . The distance between tower A and tower B is $2r_n + D$, where $D \sim Exp(\eta)$. The angle between the line joining the cluster of users and tower A and the one between towers A and B makes an angle of θ .

²Around a primary (say primary j) transmitter we can define a no-talk radius ($r_{n,j}$). Secondaries can only transmit if they are outside this no-talk radius. The size of the no-talk area depends on the level of protection that the primaries wish to have and well as the power density of the secondaries. Details of this model can be found in [9], [11].

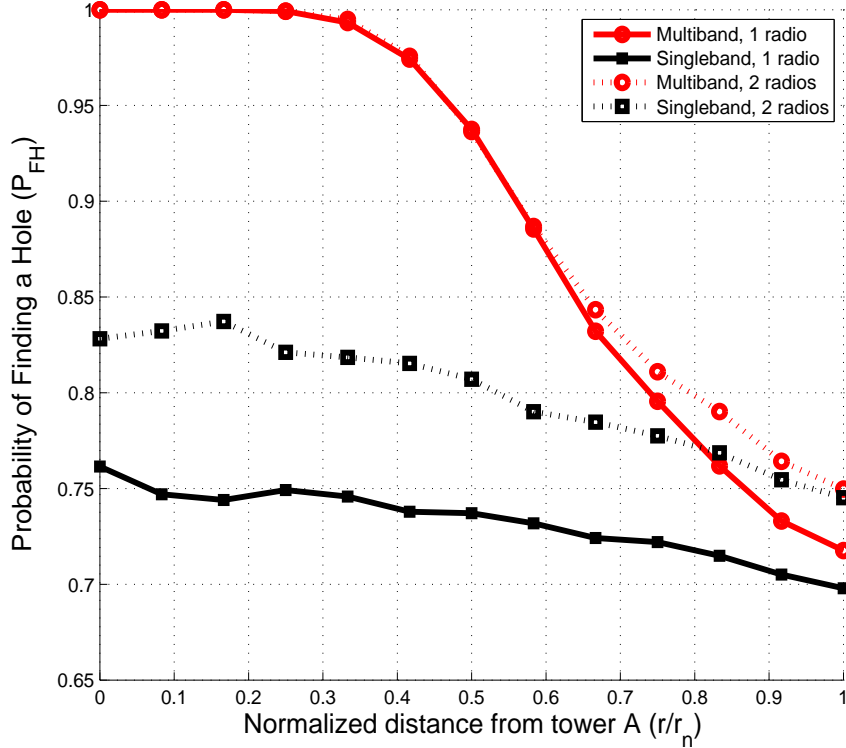


Fig. 1. Probability of finding a Hole (P_{FH}) at various distances from the tower A ($F_{HI} = .1$). The multiband algorithm performs best when closest to tower A since the signal from tower A is strongest here. Such a strong signal enables us to raise the threshold. Increasing the number of radios enables the singleband algorithm to achieve a higher P_{FH} .

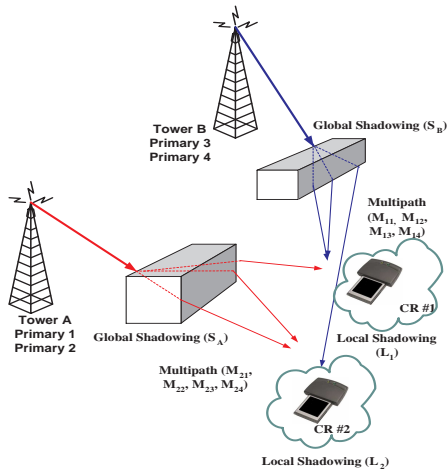


Fig. 3. Model of the fading between the towers and the cluster of users. All primaries from a given tower see the same global shadowing. Local shadowing at each radio is independent and direction agnostic. Multipath for each (radio, primary) tuple is independent for all other tuples.

B. Shadowing Model

Next we need come up with a shadowing model that reflects reality. We realize that shadowing seen by a given

radio (i) for a given primary (j) is going to be correlated to that of another radio (i') sensing the same primary (j) as well as with the same radio (i) sensing another primary (j'). Specifically the model should be true to the following facts:

- A radio sensing two co-located primaries will see similar shadowing. This fact was verified for indoor transmission in [10]. This fact is explained by the observation that variations in absorption coefficients of materials for Electro-Magnetic radiation is very small over large variations in frequency ($200 - 400MHz$).
- Multipath seen by co-located primaries is going to be essentially independent since multipath changes on the order of wavelengths.
- Two radios sensing the same primary may see correlated shadowing but will see independent multipath.

We propose the following model for shadowing that takes into account the above observations.

Let $P_{ij}(r)$ represent the received power (in dB scale) at secondary user i , for primary j at a distance r from the primary's transmitter. We use the function $T(\cdot)$ to specify the tower for channel j . So $T(j) = A$ if primary j is on tower A . With this notation, we can write P_{ij} as:

$$P_{ij}(r_{T(j)}) = 10 \log_{10}(P r_{T(j)}^\alpha) - S_{T(j)} - L_i - M_{ij} \quad (1)$$

where P is the transmit power of any given primary (we assume that the power of all the primaries is the same), $S_{T(j)}$ is the global shadowing experienced by all primaries on tower $T(j)$. L_i is a direction agnostic local shadowing around radio i . M_{ij} is the multipath experienced by radio i for the signal from Primary j . Further we assume that $M_{ij} \perp M_{i'j'}$ for $i \neq i', j \neq j'$. Similarly, $L_i \perp L_{i'}$ for $i \neq i'$ and $S_{T(j)} \perp S_{T(j')}$ for $T(j) \neq T(j')$. Furthermore, global shadowing, local shadowing and multipath are independent of each other. We also assume that shadowing and multipath are inherently attenuating process (i.e. $L_i \geq 0, M_{ij} \geq 0$ and $S_{T(j)} \geq 0$). For the purposes of the model we assume that $M_{ij} \sim \mathcal{N}(\mu_M, \sigma_M^2)$, where μ_M is large enough that $Q(\frac{-\mu_M}{\sigma_M}) \approx 1$. Similarly, $L_i \sim \mathcal{N}(\mu_L, \sigma_L^2)$, $S_{T(j)} \sim \mathcal{N}(\mu_G, \sigma_G^2)$, $Q(\frac{-\mu_G}{\sigma_G}) \approx 1$ and $Q(\frac{-\mu_L}{\sigma_L}) \approx 1$.

Hence the distribution of the received power is Gaussian with a mean that is dependent on distance.

C. Multiband Detector Design

The detection algorithm knows how many channels are on which tower (it knows C_A and C_B) but it does not the actual assignment of channels to towers (it does not know the function $T(\cdot)$). For channel j the algorithm comes up with a binary decision D_j . If D_j is 0, we are free to use the band. Similarly if D_j is 1 we are not allowed to use the band.

III. METRICS

In [9] we proposed the metrics of Fear of Harmful Interference (F_{HI}) and Probability of Finding a Hole P_{FH} to evaluate the safety and performance, respectively of any detection algorithm. These metrics have been reproduced in Appendix A for completeness. In this section we extend these metrics to the two tower multi channel case.

For simplicity we define Fear of Harmful Interference with respect to tower A . For channel j such that $T(j) = A$ we define ($F_{HI}(j)$) as:

$$F_{HI}(j) = \sup_{0 \leq r_{T(j)}} \sup_{F_r \in \mathbb{F}_{r_{T(j)}}} \mathcal{P}_{F_r}(D_j = 0 | r_{T(j)}). \quad (2)$$

where D_j is the decision of our detector for primary/channel j , $T(j)$ is the tower to which channel j belongs and $r_{T(j)}$ is the distance from tower $T(j)$. $\mathbb{F}_{r_{T(j)}}$ is the set of distributions that satisfy the primary's distribution constraints. For the remainder of the paper we shall suppress the issue with distributional uncertainty. We assume that there is a single distribution in the set $\mathbb{F}_{r_{T(j)}}$, namely $F_{r_{T(j)}}$.

As stated in Section II-B, the distribution $F_{r_{T(j)}}$ is Gaussian with a mean that depends on distance.

We would like to meet the target F_{HI} for all channels. The final F_{HI} is given by:

$$F_{HI} = \max_{1 \leq j \leq C_A} F_{HI}(j) \quad (3)$$

The maximum is over all the channels we wish to sense. Since the distribution is symmetric across channels the 'max' operation is redundant.

Next we consider a metric to deal with the secondary's performance — its ability to identify spectrum opportunities.

We define probability of finding a hole (P_{FH}) with respect to tower B . Furthermore, instead of evaluating P_{FH} at all locations on a 2-D space, we wish to evaluate P_{FH} at a distance r_A from tower A . If tower B is at a location (d, θ) from tower A we get,

$$P_{FH}(r_A, d, \theta) = \mathcal{P}_{F_{r_A, r_B}}(D_c = 0 | r_A, r_B)$$

where r_B is the distance of the cluster of users from tower B , ($r_B = \sqrt{(r_A - d \cos \theta)^2 + (d \sin \theta)^2}$) and F_{r_A, r_B} is the distribution of the fading at a location r_A from tower A and r_B from tower B .

Taking the expectation over all locations of tower B we get,

$$P_{FH}(r_k) = \mathbb{E}_{F_{D, \Theta}} P_{FH}(r_k, r_l)$$

where D is the random variable representing the distance between the two towers and d is a realization of D . Similarly, Θ is the random variable for angular position of the second tower and θ is a given realization of Θ .

Note that while these metrics have been defined with respect to specific towers we could easily extend these metrics to the case of multiple towers.

Table I compares the metrics proposed above with the metrics for single tower single channel case as proposed in [9].

IV. MULTI PRIMARY DETECTION

A. Simple Multiband Algorithm

We would like to use a simple multiband detection algorithm that utilizes the fact that being near one tower allows us to infer that we are far away from the other tower. (It must be noted that we have no knowledge of the distances between the towers or which channels are on which tower³). Furthermore, we wish to estimate the global shadowing and to use it to improve the detection of a single channel.

We propose the following simple multiband algorithm.

Sense each channel: Each radio senses each primary and determines received power (P_{ij} is the received power for radio i on channel j)

³In reality we may know which channels are on which tower e.g. we know which channels are on Sutro tower. However we do know our position relative to the towers, hence for sensing we are clueless about the assignment of the primaries.

Philosophical Idea	Single Tower Single Channel	Multi Tower Multi Channel
Safety of the primary under uncertainty.	F_{HI} for a single channel.	Worst case F_{HI} over all channels.
Performance	Recovering area outside r_n of single channel.	No. of channels recovered at location (x,y) Specifically within r_n of given tower.
Uncertainty about location of towers.	Use exponential weighting to discount placement of a second tower. Single metric - Weighted Area Recovered (WPAR)	Take expectations over placement of other towers.
Uncertainty about deployment	Use GPS measurements to reduce uncertainty in local shadowing.	Proposed multiband algorithm reduces uncertainty in local shadowing.

TABLE I

COMPARISON OF THE METRICS FOR SINGLE TOWER-SINGLE CHANNEL VERSUS THOSE FOR MULTI-TOWER MULTI-CHANNEL. THE PHILOSOPHY BEHIND THE METRICS IS THE SAME EVEN THOUGH THE ACTUAL METRICS MAY BE DIFFERENT. FOR DETAILS OF THE SINGLE-TOWER SINGLE-PRIMARY METRICS REFER TO APPENDIX A OR TO [9]. APPENDIX A ALSO EXPLAINS THE USE OF THE METRICS FOR ANALYZING THE SAFETY-PERFORMANCE TRADEOFFS OF THE ENERGY DETECTOR.

Get an estimate of global shadowing and path loss:

Compute an estimate of global shadowing and path loss as:

$$\hat{s} = \max_{i,j} P_{ij} \quad (4)$$

Compute test statistic for channel j :

$$T(j) = \max_i P_{ij} \quad (5)$$

Compute decision for each channel

$$\hat{s} - T(j) \begin{cases} \text{use channel } j & \geq \\ \text{don't use channel } j & \end{cases} B_{N,C_A}(\hat{s}) \quad (6)$$

where the $B_{N,C_A}(\cdot)$ is a function of N users and the C_A channels on tower A. Formally,

$$B_{N,C_A}(\hat{s}) = \begin{cases} 0 & \text{if } \hat{s} \leq s_1 \\ \hat{s} - \lambda_0 & \text{if } s_1 \leq \hat{s} \leq s_2 \\ K & \text{if } \hat{s} \geq s_2 \end{cases} \quad (7)$$

where λ_0, s_1, s_2 and K are design time parameters to be set to meet the target F_{HI} .

B. Analysis of the Multiband Algorithm

1) *Intuition into the Budget:* The three regions in Equation 7 correspond geometrically to different regions in Figure 2. If \hat{s} is large (i.e. our estimate of path loss and global shadowing is small) we know that we are within r_n of a tower and hence we need to budget K for the difference of the random variables $\max_{i,j} P_{ij} - \max_i P_{ij}$. On the other hand when \hat{s} is small (i.e. our estimate of path loss and global shadowing is large) we can be sure that we are way outside r_n and hence we can reduce our budget for $\max_{i,j} P_{ij} - \max_i P_{ij}$. In the intermediate region, multiband does not give us any gains and Equation 6 becomes $T(j) \geq \lambda_0$.
use channel j

This budget is shown for various scenarios in Figure 4. As discussed earlier, for some values of \hat{s} , the chance it came

from r_n is almost zero. For these values we are well either within r_n or well outside. If well inside, we need to budget for the maximum value of $\max_{i,j} P_{ij} - \max_i P_{ij}$. Intuitively this is what we would set as the value of K . Also s_1 would be set where the probability that \hat{s} came from r_n is almost zero. Similarly, if we were well outside we do not need to budget anything for $\max_{i,j} P_{ij} - \max_i P_{ij}$. where the probability that \hat{s} came from r_n is almost zero.

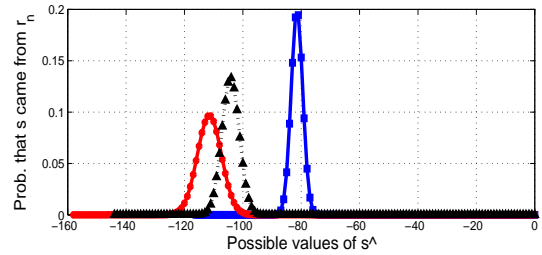
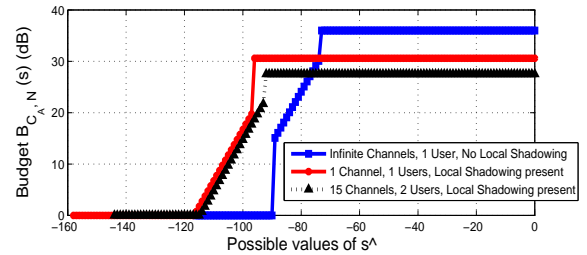


Fig. 4. Value of $B_{N,C_A}(\hat{s})$ for various values of C_A and N . The case of infinite channels and 1 user and no local shadowing is one in which Equation (4) provides an exact estimate of path loss and global shadowing. The maximum uncertainty is when we have a single user and a single channel. The uncertainty in the level of path+global shadowing is reduced as the number of channels and users is scaled.

2) *Asymptotic Performance:* In the limit of infinite channels and infinite users we are only left with global shadowing to budget for. We would like to understand how

we approach that limit with a finite number of channels and users i.e. we wish to understand the behavior of $\max_{i,j} P_{ij}$ as $N \rightarrow \infty$.

We can write $\max_{i,j} P_{ij}$ as $\max \left(\max_{i,j,T(j)=A} P_{ij}, \max_{i,j,T(j)=B} P_{ij} \right)$.

We can bound $\max_{i,j,T(j)=k} P_{ij}$ ($k = A, B$) from above as:

$$\begin{aligned} \max_{i,j,T(j)=k} P_{ij} &= \max_{i,j,T(j)=k} (10 \log_{10}(P r_k^\alpha) - S_k - L_i - M_{ij}) \\ &= 10 \log_{10}(P r_k^\alpha) - S_k + \max_{i,j,T(j)=k} (-L_i - M_{ij}) \\ &\leq 10 \log_{10}(P r_k^\alpha) - S_k + \max_i (-L_i) \\ &\quad + \max_{i,j,T(j)=k} (-M_{ij}) \end{aligned}$$

Similarly, $\max_{i,j,T(j)=k} P_{ij}$ can be bounded below as:

$$\begin{aligned} \max_{i,j,T(j)=k} P_{ij} &= \max_{i,j,T(j)=k} (10 \log_{10}(P r_k^\alpha) - S_k - L_i - M_{ij}) \\ &= 10 \log_{10}(P r_k^\alpha) - S_k \\ &\quad + \max_i (-L_i + \max_{j,T(j)=k} -M_{ij}) \\ &\geq 10 \log_{10}(P r_k^\alpha) - S_k + \max_i (-L_i - M_i) \end{aligned}$$

where M_i is a randomly chosen among all $M_{i,j,T(j)=k}$.

Since the number of channels is limited, we would like to study the scaling of $\max_{i,j,T(j)=k} P_{ij}$ with the number of users (N).

If $U_N = \max(X_1, \dots, X_N)$ where $X_i \sim \mathcal{N}(\mu, \sigma^2)$, then

$$\frac{U_N - \mu - a_N}{\sigma b_N} \xrightarrow{D} \exp(-e^{-x}) \quad (8)$$

where $a_N = (2 \log N)^{\frac{1}{2}} - \frac{\frac{1}{2} \log(4\pi \log N)}{(2 \log N)^{\frac{1}{2}}}$ and $b_N = (2 \log N)^{\frac{1}{2}}$ [12].

Hence in the limit of $N \rightarrow \infty$, the lower and upper bounds of $\frac{\max_{i,j,T(j)=k} P_{ij} - a_N - \mu_m - \mu_l - \mu_s - 10 \log_{10}(P r_k^\alpha)}{b_N}$ converge in distribution to the same random variable which has a variance given by $\frac{\pi}{6} (\sigma_m^2 + \sigma_l^2)$. Furthermore the variance of the bounds scales as $\mathcal{O}(\frac{1}{\log N})$ [12].

V. RESULTS

A. Singleband versus Multiband

In this section, we shall evaluate the performance of the multiband algorithm via simulations. Figure 1 compares the probability of finding a hole (P_{FH}) of the multiband algorithm to that of the singleband algorithm. The singleband algorithm used for channel j is the following:

$$\max_i P_{ij} \begin{matrix} \text{don't use channel } j \\ \geq \\ \text{use channel } j \end{matrix} \lambda_{SB} \quad (9)$$

where the λ_{SB} is set to meet the target F_{HI} . The parameters used in the simulation are shown in Table II.

The multiband algorithm has a significant advantage over the singleband algorithm at distances close to tower A. In these locations the signal from tower A is strong and hence the detection threshold can be set higher in a dynamic fashion. As we away from tower A, the signals grow progressively weaker and the benefits from multiband sensing degrades.

Adding a second user is clearly advantageous for the singleband algorithm - the detection threshold can be raised to increase P_{FH} while meeting F_{HI} .

The multiband algorithm already achieves a P_{FH} close to 1 near tower A and hence additional users do not provide any gains. Even at distances close to r_n there is little difference between the performance of 1 single user versus 2 users. To understand this is the case, consider the budget that we have in Equation 6. $B_{C_{A,1}}(\hat{s}) \approx B_{C_{A,2}}(\hat{s})$ for a large number of channels. Effectively, multiband acts as a proxy for increasing the number of users.

The performance in terms of P_{FH} increases significantly as we allow a larger value of Fear of Harmful Interference (F_{HI}). Figure 5 shows this improvement at various distances from tower A.

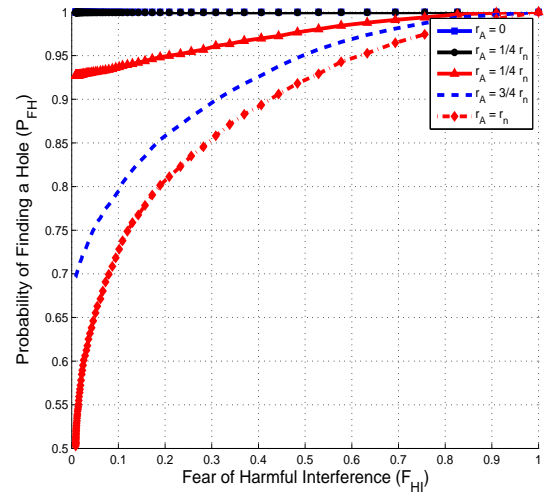


Fig. 5. Probability of Finding a Hole (P_{FH}) for various values of F_{HI} . The worse case for multiband is r_n . Here the loss is due to the budget for global shadowing and for the case that tower B may be close in.

Parameter	Description	Value used
P	Power of primary transmitter	100kW
r_n	No talk radius	60km
α	Attenuation Coefficient	-2.5
$\frac{1}{\eta} + 2r_n$	Mean distance between towers A and B	130km
μ_g	Mean of global shadowing	12dB
σ_g	Standard deviation of global shadowing	2dB
μ_l	Mean of global shadowing	12dB
σ_l	Standard deviation of local shadowing	2dB
μ_m	Mean of Multipath	18dB
σ_m	Standard deviation of Multipath	3dB

TABLE II
RELEVANT PARAMETERS AND THEIR VALUES AS USED IN THE SIMULATION SETUP.

B. Ensuring Quality of Service

As mentioned in Section I, we are interested in providing metrics that enable the Network/Link layer to provide QoS. For this reason we are interested in the average number and standard deviation of the number of channels of tower B recovered at various distances from tower A . Figure 6 shows the number of channels recovered as we scale the number of users. Increasing the number of users has a slight increase in the average but the standard deviation remains pretty high. If we had an infinite number of channels and an infinite number of users we would obtain an exact estimate for the global shadowing and pathloss. Unfortunately we cannot distinguish the two and so we still need to account for global shadowing. This limiting performance is shown in Figure 6 as the black curve with circular markers. If global shadowing is bad or if the other tower is close in then we lose all the channels at once. This effect is seen best in the histogram of channels recovered in Figure 7 at a distance r_n from tower A . When the number of channels and users is small, there are variations in the local shadowing and multipath. These variations give rise to the histogram on the left. When we scale the number of users and channels these variations vanish and we get the histogram on the right.

The ultimate performance is obtained from a genie detector - the genie knows the location of the towers and the radios. This performance is shown in Figure 6 as the blue curve with circular markers. At large distances from tower A there is a chance that we may end up within the no talk of tower B - hence the gap from C_B .

VI. CONCLUSIONS

In this paper we have presented an alternate philosophy aimed at recovering spectrum holes. Under this philosophy, detector performance is measured by safety and performance metrics of Fear of Harmful Interference (F_{HI}) and Probability of Finding a Hole (P_{FH}) respectively. These metrics match well with Network/Link layer Quality of Service guarantees. Furthermore, these metrics allow for calibrated/assisted de-

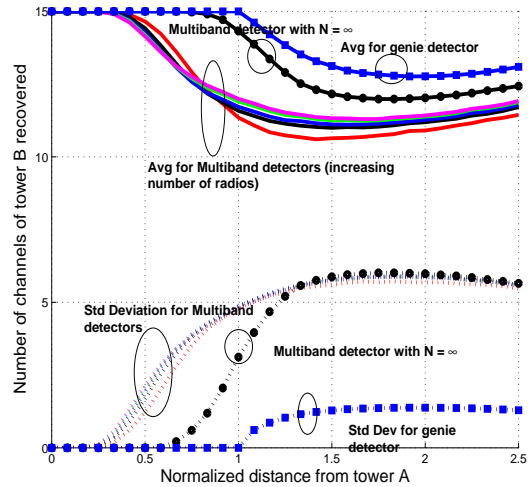


Fig. 6. We assume that there are 15 channels on each tower i.e ($C_A = C_B = 15$). The average and standard deviation of the number of channels of tower l recovered are shown. Increasing the number of radios enables us to perform better but this gain is limited by the uncertainty in global shadowing. The gap between the genie detector (one that knows its position) and the $N = \infty$ detector illustrates the gap due to global shadowing uncertainty.

tection. The simplest form of assisted detection is multiband sensing where we sense multiple channels on multiple towers. In this paper we have presented a simplified two-tower model that captures the gains from multiband sensing. The multiband sensing algorithm performs much better than the single band algorithm especially in the vicinity of a tower. The algorithm utilizes the fact that proximity to one tower enable us to declare channels on a far away tower as free.

REFERENCES

- [1] R. W. Broderson, A. Wolisz, D. Cabric, S. M. Mishra, and D. Willkomm. White paper: CORVUS: A Cognitive Radio Approach for Usage of Virtual Unlicensed Spectrum. Technical report, 2004.
- [2] Spectrum policy task force report. Technical Report 02-135, Federal Communications Commission, Nov 2002.

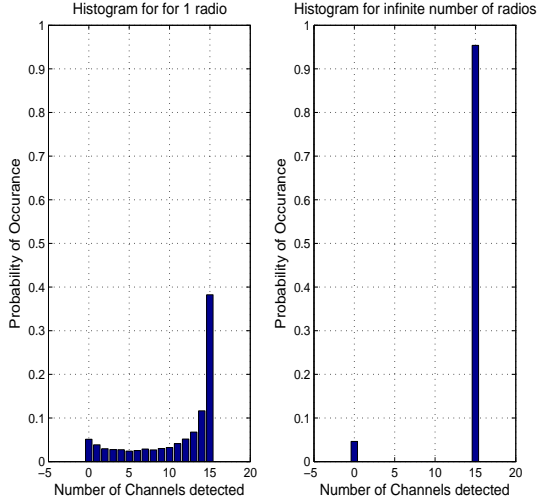


Fig. 7. (a) The histogram of the number of channels recovered for a single radio using multiband sensing. (b) The histogram of the number of channels recovered as the number of radios is scaled to ∞ . For a single radio, there can be differences between the multipath encountered by various channels. For $N = \infty$, multipath variations are essentially absent. In this case we lose all channels when global shadowing is large and recover all channels when global shadowing is small.

- [3] Dupont Circle Spectrum Utilization During Peak Hours. Technical report, The New America Foundation and The Shared Spectrum Company, 2003.
- [4] Yonghong Zeng and Ying-Chang Liang. Eigenvalue based sensing algorithms. Technical report, July 2006.
- [5] Monisha Ghosh, Vasanth Gaddam, and Gene Turkenich. DTV Signal Sensing Using Pilot Detection. Technical report, March 2007.
- [6] W. Hu, D. Willkomm, L. Chu, M. Abusubaih, J. Gross, G. Vlantis, M. Gerla, and A. Wolisz. Dynamic Frequency Hopping Communities for Efficient IEEE 802.22 Operation. *IEEE Communications Magazine, Special Issue: Cognitive Radios for Dynamic Spectrum Access*, 45(5):80–87, March 2007.
- [7] C. Cordeiro, K. Challapali, D. Birru, and Sai Shankar. IEEE 802.22: the first worldwide wireless standard based on cognitive radios. In *Proc. of the first IEEE International Symposium on New Frontiers in Dynamic Spectrum Access Networks, DySPAN*, 2005.
- [8] Digital Television/HDTV channel list: San Francisco Bay Area.
- [9] R. Tandra, S. M. Mishra, and A. Sahai. What is a Spectrum hole and what does it take to recognize one? *Submitted to the Proceedings of the IEEE*.
- [10] S. M. Mishra, R. Tandra, and A. Sahai. The case for Multiband Sensing. In *Proc. of the Allerton Conference on Communications, Control and Computing*, September 2007.
- [11] Niels Hoven. On the feasibility of cognitive radio. Master's thesis, University of California, Berkeley, 2005.
- [12] H. A. David and H. N. Nagaraja. *Order Statistics*. John Wiley and Sons Inc, 2005.
- [13] Paul Samuelson. A note on measurement of utility. *The Review of Economic Studies*, 4(2):155–161, Feb 1937.
- [14] H. Niedercorn. A Negative Exponential Model of Urban land use densities and its implications for Metropolitan Development. *Journal of Regional Science*, 11:317–326, may 1971.

APPENDIX A

SINGLE TOWER SINGLE PRIMARY CASE

A. Metrics

We define, F_{HI} for the single primary single tower case as:

$$F_{HI} = \sup_{0 \leq r \leq r_n} \sup_{F_r \in \mathbb{F}_r} \mathcal{P}_{F_r}(D = 0 | r_{actual} = r). \quad (10)$$

where D is the decision of our detector for the single primary. The outer supremum reflects the uncertainty in secondary deployments and the inner supremum reflects the uncertainty in the distribution of the fading.

Next define P_{FH} for a single tower single primary case as:

$$P_{FH}(r) = \mathcal{P}_{F_r}(D = 0 | r_{actual} = r), \quad (11)$$

where F_r is the probability distribution of the multipath and shadow fading at a distance $r \geq r_n$ from the primary transmitter.

The goal is to combine the probabilities $P_{FH}(r)$ into a single performance metric that allows a comparison among different sensing algorithms. One choice is the underlying utility of the secondary system, like the total throughput or profit. However, such holistic utility functions are intertwined with the system architecture and business models along with assumptions regarding the placement of all the primary transmitters and the population distribution. It is useful to find an approximate utility function that decouples the evaluation of the sensing approach from all of these other concerns.

We make the reasonable assumption that secondary utility will increase whenever additional area is recovered by the sensing algorithm. Since we would like to decouple the sensing metric from the detailed model for primary deployments, it is useful to be able to state it in terms of a single primary transmitter. We define the Weighted Probability of Area Recovered (WPAR) as:

$$WPAR = \int_{r_n}^{\infty} w(r) P_{FH}(r) r dr, \quad (12)$$

where $w(r)$ is a weighting function that satisfies $\int_{r_n}^{\infty} w(r) r dr = 1$.

With a single primary transmitter, the total area of the spectrum hole is infinite. For such primaries we can use discounted-area approach analogous to the present-value of consumer utility proposed by [13] i.e. $w(r) = \text{Exp}(-\tau(r - r_n))$. While similar results can be obtained for any other weighting function, the exponential weighting is not unreasonable.

- Since TV towers are often located around areas of high population density, areas around the no-talk are more valuable in terms of deploying a secondary system than areas far away. The economic value of an area is proportional to the number of potential customers there. Population densities are often modeled as decaying exponentially as one moves away from the central business district [14].
- As we move away from any specific tower, there is a

chance that we may enter the no-talk zone for another primary tower transmitting on the same frequency.

B. Performance of the Radiometer under the new metrics

The radiometer collects the samples of the received signal $Y[n]$, computes its empirical power and compares it to a detection threshold. The test-statistic for the radiometer can be written as

$$T(\mathbf{Y}) = \frac{1}{M} \sum_{m=1}^M |Y[m]|^2 \underset{D=0}{\overset{D=1}{\geq}} \lambda_0, \quad (13)$$

where λ is the design parameter and is called the detector threshold. Here, $Y[m] = X[m] + W[m]$, where $X[m]$ is the faded primary signal at time m , and $W[m]$ is the background noise at time n . For convenience assume that all $W[m]$ are independent and identically distributed as $\mathcal{N}(0, \sigma_w^2)$. Also, let M be the total number of samples that are collected for sensing.

The average power of the received primary signal is given by $P_{rx} = \lim_{M \rightarrow \infty} \frac{1}{M} \sum_{m=1}^M |X[m]|^2$. Note that P_{rx} is a random variable which changes as the shadowing and multipath environments change.

1) *Finite Sample case*: For a given target F_{HI}^t , the finite M radiometer detector chooses a value of λ_0 that maximizes its WPAR.

Mathematically,

$$\begin{aligned} F_{HI}(r) &= \mathcal{P}_{F_r} \left(\frac{1}{M} \sum_{m=1}^M |Y[m]|^2 \leq \lambda_0 \right) \\ &\stackrel{a}{=} \mathcal{P}_{F_r} \left(1 - Q \left(\frac{\lambda_0 - (\sigma_w^2 + P_{rx})}{\sqrt{\frac{2}{M}(\sigma_w^2 + P_{rx})}} \right) \right) \end{aligned}$$

where (a) follows from the fact that $\frac{1}{M} \sum_{m=1}^M |Y[m]|^2 \sim \mathcal{N}(\sigma_w^2 + P_{rx}, \frac{2}{M}(\sigma_w^2 + P_{rx})^2)$.

Similarly we can write P_{FH} and WPAR as,

$$\begin{aligned} P_{FH}(r) &= \mathcal{P}_{F_r} \left(\frac{1}{M} \sum_{m=1}^M |Y[m]|^2 \leq \lambda_0 \right) \\ &\stackrel{a}{=} \mathcal{P}_{F_r} \left(1 - Q \left(\frac{\lambda_0 - (\sigma_w^2 + P_{rx})}{\sqrt{\frac{2}{M}(\sigma_w^2 + P_{rx})}} \right) \right) \\ WPAR &= \int_{r_n}^{\infty} w(r) P_{FH}(r) r dr, \end{aligned}$$

The choice of λ_0 can be now be stated as an optimization problem,

$$\max_{\lambda_0} \int_{r_n}^{\infty} w(r) P_{FH}(r) r dr, \quad (14)$$

$$s.t. \quad \sup_{0 \leq r \leq r_n} F_{HI}(r) \leq F_{HI}^t \quad (15)$$

2) *Infinite Sample case*: In the infinite sample case, the optimization problem is easier to solve.

$$\begin{aligned} F_{HI}(r) &= \mathcal{P}_{F_r} (P_{rx} + \sigma_w^2 \leq \lambda_0) \\ &= \mathcal{P}_{F_r} (10 \log_{10}(P_{rx}) \leq 10 \log_{10}(\lambda_0 - \sigma_w^2)) \end{aligned}$$

If we assume a model for the received power to be $10 \log_{10}(P r^\alpha) - \Delta$ where $\Delta \sim \mathcal{N}(\mu_s, \sigma_s^2)$, then we can write,

$$F_{HI}(r) = 1 - Q \left(\frac{10 \log_{10}(\lambda_0 - \sigma_w^2) - 10 \log_{10}(P r^\alpha) - \mu_s}{\sigma_s} \right)$$

Since $10 \log_{10}(P r^\alpha) - \mu_s$ is a decreasing function of r , the worse case for F_{HI} is at r_n , i.e. $F_{HI} = F_{HI}(r_n)$.

From Equation (A-B2), we can obtain the value for λ_0 for any given value of F_{HI}^t .

3) *Results*: Figure 8 shows the probability of recovering spectrum at various distances from the center for a target F_{HI} of .1. As expected, conservatism leads to significant loss in spectrum recovered. This is particularly true for the finite sample radiometer.

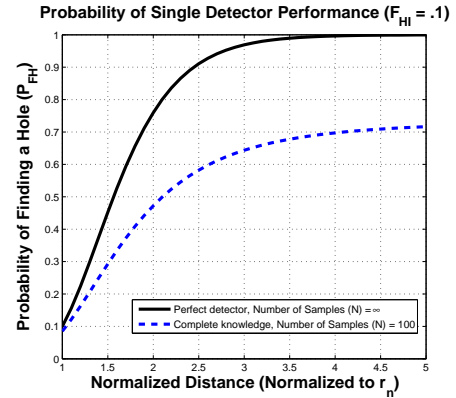


Fig. 8. Probability of Finding a Hole (P_{FH}) at various points distances from the center to meet a F_{HI} of .1. The finite sample radiometer does not recover all area even at five times the no-talk radius.

Figure 9 consolidates all the distance dependent values $P_{FH}(r)$ into a single WPAR metric. This consolidations enables us to see observe the complete tradeoff between safety and performance in a 1-D view-graph.

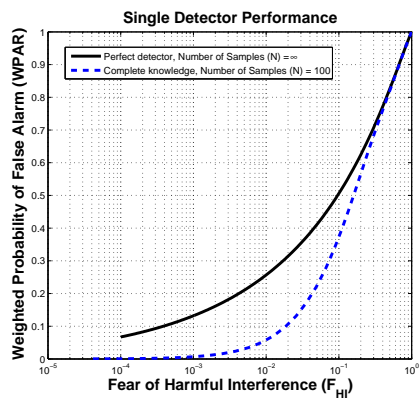


Fig. 9. Weighted Probability of Area recovered using a infinite samples for a radiometer versus using a finite sample ($M = 100$) radiometer. The spectral area recovered by both detectors is small.